

Optical Control of Ultracold Collisions in Metastable Xenon

M. Walhout, U. Sterr, C. Orzel,* M. Hoogerland, and S. L. Rolston

*Atomic Physics Division PHY A167, National Institute of Standards and Technology,
Gaithersburg, Maryland 20899*

(Received 24 August 1994)

Near-resonant light is used to modify the collision dynamics of magneto-optically trapped metastable xenon atoms. Enhanced collisional ionization occurs for a “control laser” tuned below resonance, greatly exceeding the predictions of existing models of trap loss very close to resonance. With the trapping laser off, control light tuned above resonance suppresses ionization by a factor of 8. With the trap light on, a suppression factor >30 is observed. Increases in the number and density of trapped atoms and in the trap lifetime attest to the utility of optical control of collisions.

PACS numbers: 32.80.Pj, 34.50.Fa, 34.50.Rk

Near-resonant laser light greatly modifies the collision dynamics of ultracold atoms. Collision time scales may be longer than excited-state lifetimes, so that atoms absorb and/or emit photons while colliding. The laser interaction may also shift molecular potentials by more than the atomic kinetic energy and affect the outcome of a collision. Many groups have investigated the collisional loss of atoms from laser traps [1–3]. Recently, attention has turned to optical shielding of ultracold collisions, which may lead to increased atomic densities [4,5]. We show that ionizing collisions between trapped metastable xenon (Xe^*) atoms can be modified with appropriately tuned laser light. Ionization is enhanced for light tuned below resonance and suppressed above resonance. We exploit the suppression of collisional trap loss to produce significant increases in the number and density of trapped atoms.

Xe^* is ideal for this study. Molecular interactions involving the metastable $6s[3/2]_2$ state are similar to those of the $6S_{1/2}$ ground state in Cs [6], allowing direct comparison with the well-studied alkali atom. In addition, there are important advantages in working with a metastable rare gas. Using ion detection, we can isolate a single class of collisions that cause trap loss: those leading to Penning or associative ionization (PI: $\text{Xe}^* + \text{Xe}^* \rightarrow \text{Xe} + \text{Xe}^+ + e^-$ or AI: $\text{Xe}^* + \text{Xe}^* \rightarrow \text{Xe}_2^+ + e^-$). Although ultracold collisions between pairs of ground-state Cs atoms can be difficult to observe, we easily detect ions from the analogous collisions between Xe^* atoms. We are therefore not restricted to studying processes that involve laser excitation. Finally, Xe isotopes with even mass number have no nuclear spin, so hyperfine structure does not affect collisions—a great simplification over experiments in alkali atom traps [7].

Our experiments utilize a magneto-optical trap (MOT) for Xe^* [8]. The magnetic field gradient in the trap is 0.5 mT/cm, and the MOT laser beams are tuned 8 MHz (1.6 linewidths) below the $6s[3/2]_2 \rightarrow 6p[5/2]_3$ laser-cooling transition at 882 nm, each with an intensity of ~ 4 mW/cm². Acousto-optic modulators are used to switch the MOT light with a 150 μ s period and an

“on” duty factor of $\frac{2}{3}$. The trapped atom cloud has an approximately Gaussian density distribution with an rms radius of ~ 80 μ m and a peak density of $\sim 5 \times 10^{10}$ cm⁻³. The background gas in the MOT vacuum chamber is predominantly Xe at a pressure of 8×10^{-7} Pa.

Collisions in the trap produce ions at a rate

$$R_i = \alpha_i N + \frac{\beta_i}{2} \int n(\mathbf{r})^2 d^3r, \quad (1)$$

where N is the number of trapped atoms, $n(\mathbf{r})$ is the atomic density distribution, α_i arises from collisions with background gas, and β_i characterizes PI and AI. The factor of $\frac{1}{2}$ appearing with β_i accounts for the two atoms lost in each AI or PI event. Though ionization is the dominant loss mechanism in the MOT, atoms are also lost through nonionizing collisions governed by rate constants α_{ni} and β_{ni} . The combined rate constant for inelastic collisions between trapped atoms, $\beta = \beta_i + \beta_{ni}$, limits the density in the MOT. Here we demonstrate the possibility of “controlling” β with near-resonant light.

To determine N and $n(\mathbf{r})$, we turn off the MOT light and fields, and after a short (200 μ s) delay, illuminate the atomic cloud for 50 μ s with a resonant laser beam much larger in diameter than the cloud. The atoms absorb light from the probe, leaving a shadow that we image on a charge-coupled-device camera. The absorption image is divided by an image obtained without trapped atoms. This procedure yields a 2D spatial profile of the optical thickness of the trap, which we fit with a 2D Gaussian function. Assuming the trap radius along the probe direction is equal to the mean radius found from the image, we calculate a 3D Gaussian atomic density profile with maximum density n_0 . To minimize uncertainties, we adjust the MOT beam alignment until the cloud has approximately spherical symmetry. The integrated density gives the number of trapped atoms N , and the integral of $n(\mathbf{r})^2$ in Eq. (1) reduces to $n_0 N / 2^{3/2}$.

The method of imaged absorption is also used to measure the atomic velocity distribution. Lengthening the delay between the MOT turn-off and the probe laser pulse,

we obtain images of the freely expanding cloud. A comparison of images at short and long delays gives the rms velocity v_{rms} . For the data presented here, v_{rms} is typically 7–8 cm/s ($T \sim 100 \mu\text{K}$).

We estimate our ion detection efficiency ε by counting the number of detected ions and the change in N during a 50 ms interval after MOT loading is turned off. On average, for every ten atoms lost from the trap, one ion is detected, giving a lower limit of 0.2 for ε . As discussed below, trap loss at short times and high densities is dominated by PI and AI ($\beta_i \gg \beta_{ni}$), so ε must be close to this limit.

In a preliminary experiment with ^{132}Xe , we vary n_0 and measure the ion rate $R_i^{(\text{dark})}$ during the trap-off intervals of the MOT chopping cycle. Inserting a Gaussian $n(\mathbf{r})$ into Eq. (1), one finds that a plot of R_i/N vs n_0 is a line with intercept α_i and slope $\beta_i/2^{5/2}$. This functional form fits well to data obtained over the range of densities $3 \times 10^9 < n_0 < 3 \times 10^{10} \text{ cm}^{-3}$. The fit intercept and slope give $\alpha_i^{(\text{dark})} = 3(2) \times 10^{-3} \text{ s}^{-1}$ and $\beta_i^{(\text{dark})} = 6(2) \times 10^{-11} \text{ cm}^3/\text{s}$, where we assume $\varepsilon = 0.2$ and quote 1-standard-deviation statistical uncertainties. For typical densities, background gas collisions contribute at most a few percent of the ion rate. The α_i term in Eq. (1) may therefore be neglected unless β_i is extremely small. We will obtain β_i assuming $\alpha_i = 0$.

To induce changes in β_i , we use a ‘‘control’’ laser beam from a Ti:sapphire laser tuned near the laser-cooling resonance. Control light is applied for 50 μs during alternate MOT-off intervals, producing a modified ion rate $R_i^{(\text{c})}$, which we measure in the last 20 μs of each interval. We also measure the rate $R_i^{(\text{dark})}$ when both MOT and control beams are off. Taking the ratio of the two rates, we obtain $\beta_i^{(\text{c})}/\beta_i^{(\text{dark})}$, which is independent of density and number fluctuations occurring on time scales longer than 150 μs . Since we have measured $\beta_i^{(\text{dark})}$, this ratio determines $\beta_i^{(\text{c})}$.

Figure 1 shows a plot of $\beta_i^{(\text{c})}$ vs control laser detuning ($\delta = \nu_{\text{control}} - \nu_{\text{atom}}$) obtained with a collimated, linearly polarized, traveling-wave control laser beam with intensity $I = 1 \text{ mW}/\text{cm}^2$ [9]. Independent data sets shown for ^{132}Xe and ^{136}Xe behave identically (assuming $\beta_i^{(\text{dark})}$ is the same for both isotopes). We find that $\beta_i^{(\text{c})}$ is enhanced with respect to $\beta_i^{(\text{dark})}$ below resonance, with a peak at -20 MHz . Above resonance, in the range $0 \leq \delta \leq 50 \text{ MHz}$, the rate is suppressed by a factor of $\beta_i^{(\text{dark})}/\beta_i^{(\text{c})} = 1.7$. Increasing the intensity of the control laser beam broadens and increases the sizes of the enhancement and suppression features. The suppression factor eventually saturates, reaching a peak value of ~ 5 near $\delta = 200 \text{ MHz}$ for $I = 0.5 \text{ W}/\text{cm}^2$. For circular polarization the suppression factor saturates at a value of ~ 8 (this is a minimum value, since α_i may contribute to R_i when β_i is suppressed far below $\beta_i^{(\text{dark})}$). Increased sup-

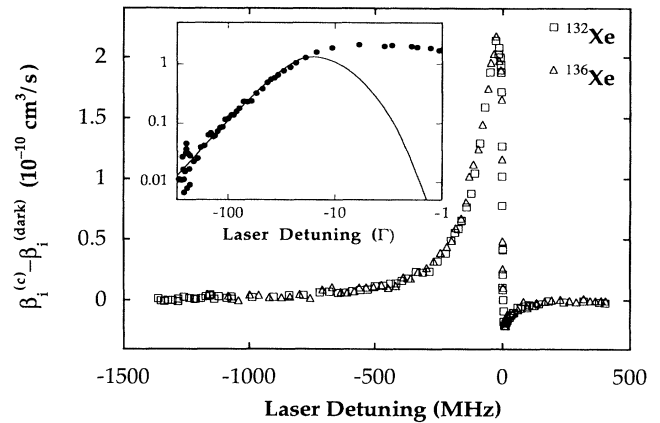


FIG. 1. The laser-induced rate coefficient $\beta_i^{(\text{c})} - \beta_i^{(\text{dark})}$ vs control laser detuning δ for $I = 1 \text{ mW}/\text{cm}^2$. The inset shows a log-log plot of the experimental data and a scaled quantum-mechanical model of Cs trap loss [12] (natural linewidth $\Gamma = 5 \text{ MHz}$).

pression due to intense, circularly polarized light may be caused by optical pumping that orients the sample, making PI or AI unlikely [10]. This explanation is consistent with an observed decrease in the enhancement of $\beta_i^{(\text{c})}$ below resonance for circular polarization. Henceforth we will discuss only linearly polarized control light, which cannot produce orientation. We note that results for ^{131}Xe (nuclear spin $= \frac{3}{2}$) resemble those for the even isotopes, but have a $\sim 40\%$ smaller peak value of $\beta_i^{(\text{c})}/\beta_i^{(\text{dark})}$ below resonance. Since $\beta_i^{(\text{dark})}$ for ^{131}Xe is unknown, we do not report the size of $\beta_i^{(\text{c})}$.

To explain the features of Fig. 1, we consider two atoms with internuclear separation R interacting on a molecular potential described at long range by a power series $\sum_n C_n/R^n$. The potential V_{ss} for two atoms in the $6s[3/2]_2$ state is dominated by $n = 5$ and $n = 6$ terms describing quadrupole-quadrupole and van der Waals interactions, respectively. Atoms reaching small R on V_{ss} can make transitions to ionic potentials corresponding to PI or AI. This mechanism accounts for $\beta_i^{(\text{dark})}$.

In the presence of light with $\delta < 0$, atom pairs are excited to a long-range, attractive potential $V_{sp}(R) = -C_3/R^3$, which arises from the dipole-dipole interaction between the $6s[3/2]_2$ and $6p[5/2]_3$ states (see Fig. 2, inset). V_{sp} accelerates atoms toward small R , where PI and AI occur. Resonant excitation occurs near the ‘‘Condon radius’’ R_C , where the energy of a control-laser photon is equal to the energy difference between V_{sp} and V_{ss} . For large negative detunings ($\delta < -50 \text{ MHz}$), the acceleration is so large that atoms reach small R in a time short compared with the natural decay time. Therefore, the enhancement in β_i is simply proportional to the probability that two atoms have separation R_C . The $1/\delta^2$ dependence of this probability is expected to

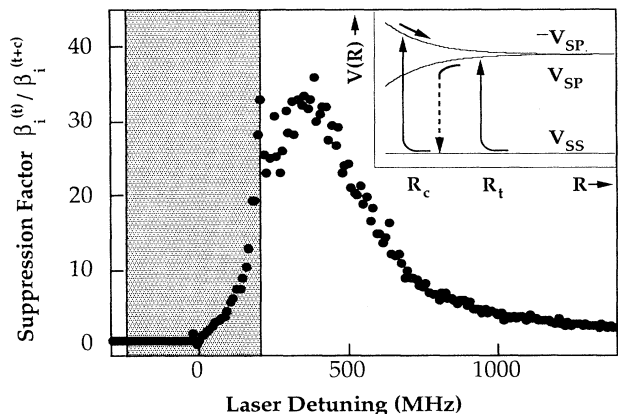


FIG. 2. Measured suppression factor vs δ for ^{132}Xe in the presence of MOT light. In the shaded region the trap is distorted by the control laser. The inset shows the shielding mechanism discussed in the text.

characterize collisional trap loss at large δ , unless atoms execute multiple oscillations on the excited potential [11–13]. As shown in Fig. 1, our data agree with calculations of $1/\delta^2$ behavior, consistent with a near-100% ionization probability at small R .

Since there is no existing ultracold collision theory for Xe^* , we compare our results to a quantum-mechanical theory for Cs [12], which considers trap loss due only to atoms reaching small R on the excited 0_u^+ molecular potential. When scaled to agree with our data at large δ , the theory curve in the inset of Fig. 1 disagrees with the experiment at small δ . Near resonance, where R_c becomes large, a drop in the enhancement curve is predicted because the short-lived excited state decays before atoms reach small R . The observed large rate for small δ may arise in part from excitation to a long-lived state analogous to the $2u$ state in Cs_2 , which could survive during acceleration to small R . However, such a state alone cannot explain the entire spectrum [14]. Saturation effects not included in [12] may also play a role, enabling reexcitation to and ionization from V_{sp} after atoms undergo the excitation-acceleration-decay process [14]. In addition to these explanations (which would also apply to alkali atom trap loss experiments), we note that ionization at small δ may be enhanced through the V_{ss} channel if acceleration on V_{sp} is followed by spontaneous decay. Even if the gradient of V_{sp} is small, there can be considerable acceleration after multiple excitation-decay cycles [9]. The energy gained may be sufficient for atom pairs with high relative angular momenta to penetrate centrifugal barriers and reach small R [15]. The relative contributions of these various mechanisms have yet to be addressed theoretically.

The suppression of β_i above resonance is explained by excitation to a long-range repulsive potential with the form $-V_{sp}$. Repulsion prevents atoms from ever reach-

ing small R and ionizing. This shielding of collisions is described for two-level atoms in 1D by the theory of [5]. For the conditions of our experiment, the theory predicts suppression factors much larger than those observed. Resolving the discrepancy may require multiple molecular states to be considered and a treatment of the problem in 3D.

Since suppressing collisional trap loss is a promising method for increasing the density and number of atoms in a MOT, controlling β in the presence of MOT light is of interest. For typical conditions, the red-detuned trap radiation produces a rate constant $\beta_i^{(t)}$ that is ~ 20 times larger than $\beta_i^{(\text{dark})}$. Adding the control laser to the trap yields a modified rate constant $\beta_i^{(t+c)}$. We now examine the suppression factor $\beta_i^{(t)}/\beta_i^{(t+c)}$ as a function of control-laser detuning. The ratio of β_i 's is obtained as in the previous experiment, except that the MOT light is left on continuously. Figure 2 shows the suppression factor vs δ for a control laser beam with $I \approx 1 \text{ W/cm}^2$. We find a peak suppression factor of >30 , corresponding to $\beta_i^{(t+c)} < 0.6\beta_i^{(\text{dark})}$.

To explain shielding in the presence of trap light, we refer to the inset of Fig. 2. Since trapping light has a small negative detuning, it excites atom pairs to V_{sp} at a large radius R_t . Acceleration may occur until the MOT laser is no longer resonant and atoms cannot be reexcited after decaying to V_{ss} . At the control-laser Condon radius ($R_c < R_t$), a pair may be excited to the repulsive potential, which shields the impending collision. Because of the high relative velocity gained in acceleration, atoms do not spend much time near R_c , which may explain the high control-laser intensities necessary for efficient shielding. The high-intensity regime may be modeled in a basis of molecular states dressed by a two-color laser field. We find that the simple system of dressed V_{ss} and $\pm V_{sp}$ potentials can indeed have repulsive barriers in the energies of states with predominately V_{ss} character at large R . Including effects of spontaneous emission in this system should enable a calculation of the shielding factor. Until such a model is available, the factor of ~ 6 difference between the MOT-on and MOT-off suppression factors remains an open question.

In the experiments presented up to this point, no significant change in n_0 or N was seen because the control laser was applied only one-sixth of the time. We now turn to an experiment in which the MOT and control lasers are left on continuously, so that the trap-loss rate constant β is significantly reduced, and the number and density of atoms in the MOT are increased. In measuring β , we monitor the MOT fluorescence intensity, which is proportional to the number of trapped atoms. With this signal calibrated by a measurement of N , we turn off the MOT loading and observe the fluorescence decay. The rate constant for background gas collisions, $\alpha = \alpha_i + \alpha_{ni}$, is found at long times, when the density

dependent loss is small. β is obtained from the initial decay rate and measured values of the initial n_0 and N .

Data from three trap-decay measurements appear in Fig. 3. Curve (a) corresponds to a trap decaying in the absence of a suppressing laser. Using the same trapping parameters, we add a control laser with $I = 300$ mW/cm², obtaining (b) with $\delta = 300$ MHz and (c) with $\delta = 165$ MHz. For (b) we measure a 40% reduction in β , and >30% increases in both n_0 and N . In (c) we find that β is suppressed by a factor of 3 and N grows by a factor >3, although n_0 decreases by nearly 50%. In an additional measurement for $I = 15$ mW/cm² and $\delta = 70$ MHz, we have seen 50% and 100% increases in n_0 and N , respectively. Note that the density-limiting forces described in [16] may enter in these experiments.

Changes observed in β are smaller (by at most a factor of 3) than those seen in $\beta_i^{(t)}$ for similar control laser parameters. The difference may arise because heating is increased with the control beam on continuously, raising the collision rate. [For the examples above, we measure a v_{rms} that is twice as large in (c) as in (a).] It is also possible that we fail to shield collisions that do not produce ions. However, such collisions are unlikely to contribute to β at the $>10^{-10}$ cm³/s level. First, in the course of measuring the $6s[3/2]_2$ lifetime [17], we obtained an estimate of the rate constant for collisions that induce changes in the fine-structure state and result in vacuum ultraviolet (vuv) photon emission. In the presence of MOT light, the density dependence of the vuv rate yields $\beta_{\text{fs}} \sim 3 \times 10^{-11}$ cm³/s. In addition, one might assume that contributions to β other than $\beta_i^{(t)}$ and β_{fs} are similar to those from Cs trap loss measurements, which also fall in the 10^{-11} cm³/s range [18].

In conclusion, we have used near-resonant light to control inelastic collisions between ultracold atoms. This

technique may be generally useful for increasing the number and density of atoms in traps. Our results are the first to enable a comparison with theory at small red detunings, where the effects of spontaneous emission are crucial. They do not agree with calculations that assume trap loss to occur only when colliding atoms reach small internuclear separations on short-lived, excited molecular states. Resolution of the disagreement will require theories to include ionization from $s + s$ potentials and/or the possible contributions of long-lived excited states. Such analyses would provide further understanding of the collisional loss mechanisms in alkali and metastable atom traps. Consideration of multilevel atoms dressed by one or two laser frequencies would also be useful in accurately estimating the degree to which collisions can be shielded.

We thank W.D. Phillips, P.D. Lett, P. Julienne, C. Williams, and F. Shimizu for helpful discussions. U.S. acknowledges funding from the Alexander von Humboldt Foundation. C.O. is supported by a UMCP/NIST Joint Fellowship in AMO Physics. This work was supported in part by the Office of Naval Research.

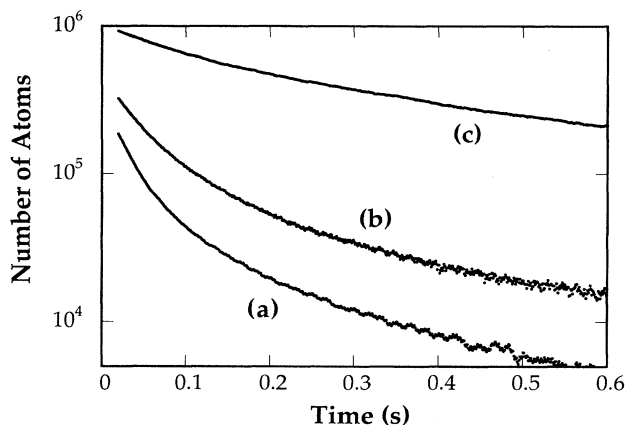


FIG. 3. Trap fluorescence decay curves (¹³²Xe). (a) No control laser: $\beta = 2.5(3) \times 10^{-9}$ cm³/s, $n_0 = 2.6(2) \times 10^{10}$ cm⁻³. (b) $I = 300$ mW/cm², $\delta = 300$ MHz: $\beta = 1.5(2) \times 10^{-9}$ cm³/s, $n_0 = 3.7(3) \times 10^{10}$ cm⁻³. (c) $I = 300$ mW/cm², $\delta = 165$ MHz: $\beta = 8(1) \times 10^{-10}$ cm³/s, $n_0 = 1.5(2) \times 10^{10}$ cm⁻³.

*Permanent address: Chemical Physics Program, University of Maryland, College Park, MD 20742-2431.

- [1] F. Bardou *et al.*, *Europhys. Lett.* **20**, 681 (1992).
- [2] D. Hoffman, P. Feng, R. Williamson, and T. Walker, *Phys. Rev. Lett.* **69**, 753 (1992).
- [3] C.D. Wallace *et al.*, *Phys. Rev. Lett.* **69**, 897 (1992).
- [4] L. Marcassa *et al.*, *Phys. Rev. Lett.* **73**, 1911 (1994).
- [5] K.-A. Suominen and P. Julienne (to be published).
- [6] A. J. Yencha, in *Electron Spectroscopy: Theory, Techniques and Application C*, edited by R. Bundle and A. D. Baker (Academic Press, London, 1984), Vol. 5, p. 197.
- [7] M.E. Wagshul *et al.*, *Phys. Rev. Lett.* **70**, 2074 (1993).
- [8] M. Walhout, H. J. L. Megens, A. Witte, and S. L. Rolston, *Phys. Rev. A* **48**, R879 (1993).
- [9] H. Katori and F. Shimizu have submitted similar results for publication.
- [10] J.C. Hill, L.L. Hatfield, N.D. Stockwell, and G.K. Walters, *Phys. Rev. A* **5**, 189 (1972).
- [11] M.G. Peters, D. Hoffman, J.D. Tobiasson, and T. Walker, *Phys. Rev. A* **50**, R906 (1994).
- [12] H.M.J.M. Boesten and B.J. Verhaar, *Phys. Rev. A* **49**, 4240 (1994).
- [13] A. Gallagher and D. Pritchard, *Phys. Rev. Lett.* **63**, 957 (1989).
- [14] P. Julienne and C. Williams (private communication).
- [15] P. Gould (private communication).
- [16] D. Sesko, T. Walker, and C. Wieman, *J. Opt. Soc. Am. B* **8**, 946 (1991).
- [17] M. Walhout, A. Witte, and S. L. Rolston, *Phys. Rev. Lett.* **72**, 2843 (1994).
- [18] D. Sesko *et al.*, *Phys. Rev. Lett.* **63**, 961 (1989).